END

DATE
FILMED

5-77

1.0

4.5
5.0
5.6

2.8

2.5

3.2

2.2

3.6

1.1

4.0

2.0

1.8

1.25

1.4

1.6

MICROCOPY RESOLUTION TEST CHART

NATIONAL BUREAU OF STANDARDS-1963-A

AFOSR - TR - 77 - 0446

ADA038625
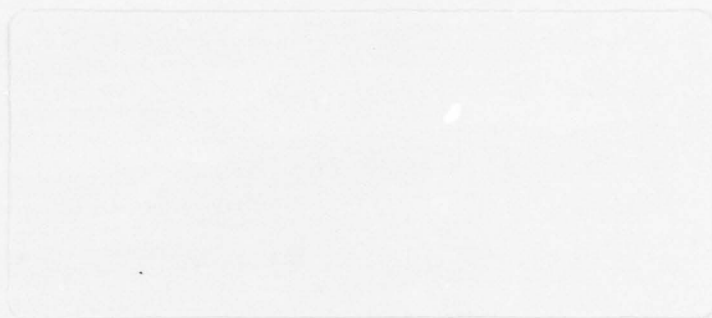
DDC

APR 25 1977

C

AD No.
DDC FILE COPY

General Applied Science Laboratories inc.

AIR FORCE OFFICE OF SCIENTIFIC RESEARCH (AFSC)
NOTICE OF TRANSMITTAL TO DDC
This technical report has been reviewed and is
approved for public release IAW AFR 190-12 (7b).
Distribution is unlimited.
A. D. BLOSE
Technical Information Officer

MARCH 1977

GASL TR 237

THE EFFECTS OF VISCOUS INTERACTION ON

THE TRANSONIC JET-FLAP

BY

P. Baronti, S. Elzweig & G. Miller

A FINAL REPORT

PREPARED FOR

AIR FORCE OFFICE OF SCIENTIFIC RESEARCH
BOLLING AIR FORCE BASE
WASHINGTON, D. C. 20332

UNDER

CONTRACT NO. F44620-76-C-0017

By

GENERAL APPLIED SCIENCE LABORATORIES, INC.
Merrick and Stewart Avenues
Westbury, New York 11590

ABSTRACT

The inviscid and viscous effects associated with a jet-flapped airfoil in
the transonic regime are investigated. The particular formulation developed
employs integral methods for the description of the viscous portions of the
flow (utilizing the turbulent kinetic energy equation) and a relaxation method
for the inviscid portions. The viscous-inviscid coupling procedures along the
wing and the jet acknowledge the importance and magnitude of the viscous ef-
fects on pressure distribution and directly incorporate the displacement ef-
fect on the wing and the effects of the jet mixing into the boundary conditions
for the computation of the entire flow. Some numerical results are presented
to validate the solution techniques that have been selected and to assess the
importance of mass and momentum entrainment into the jet on jet flap effective-
ness.

INDEX

LIST OF FIGURES

LIST OF SYMBOLS

a	speed of sound
a_i, G, L	Bradshaw turbulent parameters
c	airfoil chord
c_f	skin friction coefficient
c_p	pressure coefficient
c_j	jet momentum coefficient
$f(x)$	airfoil shape
M_∞	free stream Mach number
p	static pressure
P	wake function
q	total velocity
R	local radius of curvature of jet flap
s, n	natural coordinates
u, v	velocity components
U_∞	free stream velocity
x, y	Cartesian coordinates
α	angle of attack of wing, also stretching parameter
β	functional form, Equation (19)
Γ	circulation
δ	boundary layer thickness
δ^*	boundary layer displacement thickness
θ	angle related to jet curvature, Figure (2)
ν	relaxation step
ξ, η	stretched coordinates
π	Coles wake parameter

LIST OF SYMBOLS (Continued)

ρ density

τ initial jet flap angle, also shear stress

ϕ perturbation potential

ψ stream function

SUBSCRIPTS AND SUPERSCRIPTS

e   condition at boundary layer edge

j   jet flap

ℓ airfoil lower surface

u   airfoil upper surface

B   lower side of jet sheet

T   upper side of jet sheet

LE   leading edge

TE   trailing edge

o   condition along base line of jet

1,2   conditions at upper and lower boundary of jet

—   transformed variables

SECTION I
INTRODUCTION

The use of jet flaps to enhance maneuverability in transonic flight has been under scrutiny in recent years. Wind tunnel experiments on jet-flapped air-foils [1,2,3,4,5] have indicated that significant lift augmentation and improvement of the drag polar at large lift can be obtained in the transonic regime; at the same time, retardation of boundary layer separation and of buffet onset can be achieved. A body of theoretical work is also available which provides a mathematical and numerical framework for the solution of the transonic inviscid flow field around jet-flapped airfoils. Ives and Melnick[6] have numerically solved the full transonic potential equation while allowing the jet flap to maintain a constant, finite, thickness. Malmuth and Murphy have given a linearized solution for two-dimensional[7] and three-dimensional[8] jet-flapped wings with infinitely thin jets. However, none of these analytical models has explored the viscous effects of the jet on airfoil performance, since jet mixing has been excluded and the jet momentum assumed constant along the jet. As originally indicated by Stratford,[9] the effect of entrainment is to cause the jet to act like a sink with respect to the inviscid field, with consequent loss of recoverable jet thrust. More recently, Yoshihara and Zonars[10] have reviewed, although qualitatively, the effects of jet viscosity on jet flap performance in the transonic regime. They have pointed out, on the basis of experimental evidence, several important phenomena: the ejector action of the jet in increasing trailing edge suction (and thus decreasing thrust recovery), the effective reduction of the jet exit angle because of jet mixing, and the importance of jet and wake viscous-inviscid interaction in providing a realistic picture of the transonic flow field for large jet deflection angles.

For these reasons, an effort to assess the effects of viscous-inviscid interaction on jet effectiveness was initated by the authors in Reference (11). An inviscid analysis, as well as an attendant computer program similar to that of Ives and Melnick, was developed. In addition, integral techniques for the separate analyses of the viscous regions along the airfoil and the jet were developed and the coupling procedures outlined. The choice of an integral

method, rather than a finite difference technique, was prompted by previous work[12] which showed that boundary layers over supercritical wings and wakes can be well treated by integral methods, once implemented by a solution of the turbulent kinetic energy equation. Also, the separation of the flow into inviscid and viscous regions greatly reduces the numerical/computational effort as compared to time-dependent solutions of the "turbulent" Navier-Stokes equations, which may be foreseeably attempted in the future.

In the present report, the integral solution of the viscous flow along the jet and the viscous-inviscid coupling along the jet have been reconsidered. Further numerical experimentation has in fact revealed that the integral solution of the viscous flow along the jet developed in Reference (11) was unstable when the jet was highly curved. This has necessitated the reformulation of the momentum integral equations in terms of velocity profiles expressed by polynomials of second degree (instead of third degree, as it was originally proposed in Reference (11)). In addition, a more consistent viscous-inviscid coupling procedure along the jet has been elaborated.

The present report completes the formulation of the problem of viscous-inviscid interaction along jet-flapped airfoils, initiated in Reference (11). The salient features of the method are reviewed here. They consist of an inviscid relaxation procedure that resembles that of Ives and Melnick, integral methods for the description of the viscous (turbulent) portions of the flow along the airfoil and along the curved jet, and an appropriate coupling procedure for the treatment of the viscous-inviscid interaction along the wing and along the jet.

The integral solution of the jet flap presented here suffers from some limitations, since it requires a modelling of the viscous jet flap which may not always be consistent with physical reality. In fact, the present representation of the velocity field at the wing trailing edge or equivalently at the jet exit, considers only the jet velocity profile and disregards the detailed velocity profiles of the boundary layers on both sides of the wing which merge with the

jet flow (however, in the actual computations performed here, the initial jet profile is modified so as to satisfy, on the average, the mass and momentum flux of the jet-boundary layer combination). This representation is realistic when the boundary layer on the wing is thin and attached, or when it has very small separated regions at the wing trailing edge, but it becomes invalid in the case of jets with large initial deflection angles which may induce boundary layer separation and large recirculation regions at the wing trailing edge.[10] Notwithstanding these limitations it appears, however, that the integral representation may be usefully and simply invoked for a quantitative determination of viscous effects on jet-flap performance in many configurations of practical interest.

The report is organized as follows. In Section II the integral analysis of the viscous region along a curved jet is presented. Section III outlines the inviscid analysis and the coupling procedure of the viscous and inviscid solutions along the wing and along the jet. Some numerical results, indicating the effects of jet-mixing and entrainment on the pressure distribution over a two-dimensional airfoil, as well as some conclusions with respect to the quantitative effect of jet momentum and deflection angle, are presented in Section IV.

SECTION II

INTEGRAL METHOD FOR VISCOUS JET SOLUTION

The authors have developed in Reference (11) an integral solution of the vis-
cous flow along a curved jet. An integral solution of the boundary layer flow
over an airfoil, under subcritical and supercritical conditions, had been
previously developed in Reference (12). Both solutions utilize an integral so-
lution of the turbulent kinetic energy equation[13] and simple coordinate trans-
formations to account for compressibility effects. The formulation of the in-
tegral solution of the viscous region along a curved jet is now reconsidered.

With reference to Figure (1), a jet is issued from the trailing edge of an air-
foil with a deflection angle τ. The flow around the wing is assumed to be in-
viscid (thus the boundary layer over the wing is neglected) and only the mixing
of the jet with the inviscid flow field is considered. A line s, not neces-
sarily the centerline of the mixing region, is selected as a "base" streamline
of the flow. Its position, to be determined by the viscous-inviscid coupling
discussed below, can be proved[14] to be accurate to order δ of boundary layer
theory. Along this streamline $v = 0$, but, still within the accuracy of bound-
ary layer theory, the velocity profile $u(n)$ may have a slope different from
zero. Thus, a shear different from zero is allowed along the s-streamline.
The mixing boundaries of the curved jet, defined by the boundary lines $n=\delta_1$
and $n=\delta_2$, are asymmetric with respect to the "base" streamline and the invis-
cid velocities u_1 and u_2 along δ_1 and δ_2 are, in general, different from each
other. The problem solution requires a representation of velocity and shear
profiles which accounts for these asymmetries.

In Reference (11), the velocity profiles were represented by the third degree
polynomial

$$u = u_0 + a_1 n + a_2 n^2 + a_3 n^3$$

with the coefficients a_1 and a_2 defined by satisfying the boundary conditions
$u = u_1$ at $n = \delta_1$ and $u = u_2$ at $n = \delta_2$ (note that the edge derivatives are left
unspecified). The flow development was then defined in terms of the dependent
variable $u_0(s)$, $\delta_1(s)$, $\delta_2(s)$ and $a_3(s)$. These were obtained by integrating the
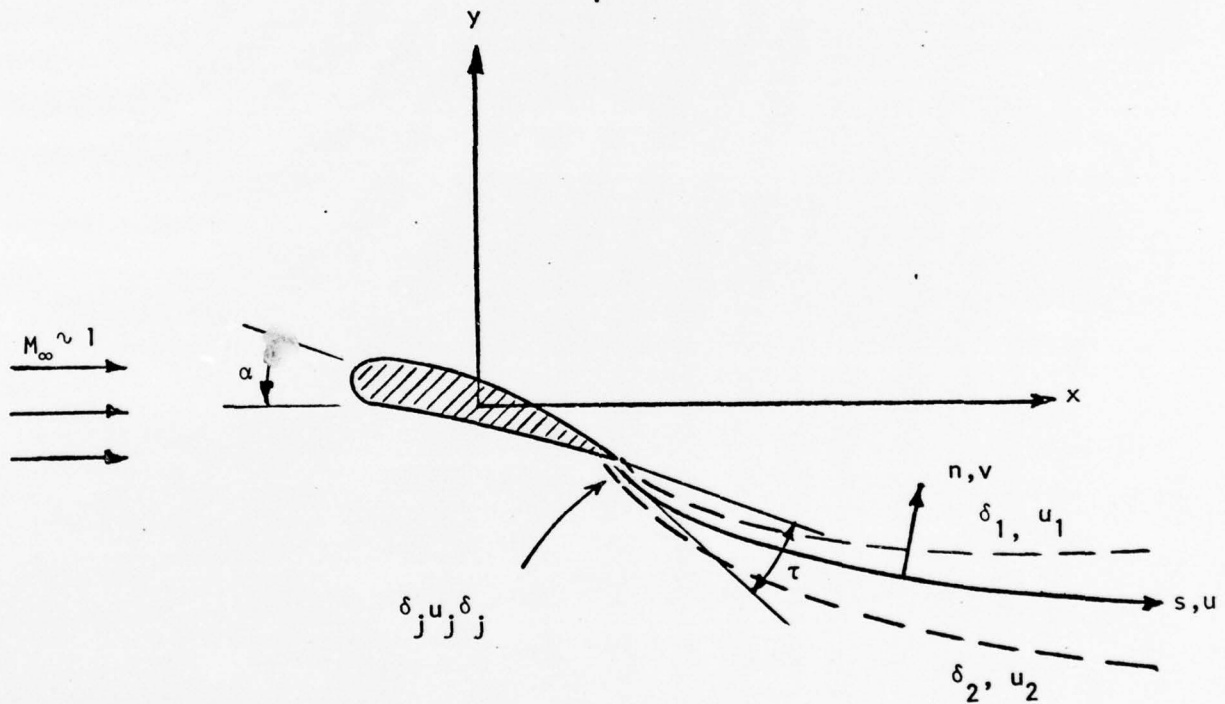
FIGURE 1. THE VISCOUS FLOW FIELD ALONG A CURVED JET FLAP

streamwise momentum equation four times, that is from the "base" streamline $n = 0$ to $\delta_1/2$ and to δ_1 and from $n = 0$ to $\delta_2/2$ and to δ_2. In a similar fashion, in order to obtain the shear distribution across the boundary layer (needed in the integration of the momentum equation), shear profiles were prescribed by the fourth order polynomial

$$\tau = b_0 + b_1 n + b_2 n^2 + b_3 n^3 + b_4 n^4$$

with the coefficients b_1, b_2 and b_0 obtained by satisfying the conditions $\tau = 0$ at $n = \delta_1$ and $n = \delta_2$ and by satisfying the s-momentum equation along the base streamline. The coefficients b_3 and b_4 were then obtained by integrating twice the turbulent kinetic energy equation of Bradshaw, Ferris and Atwell[15] between $n = 0$ and δ_1 and between $n = 0$ and δ_2.

The resulting system of integral momentum equations was analyzed extensively for asymmetric jet flows but was found to be unstable for cases of large deflection angles and large differences between $u_1(s)$ and $u_2(s)$. The instabilities were traced to the representation of the velocity profiles by polynomials of the third degree, which could produce negative velocities and uncontrolled velocity amplifications. A representation of velocity and shear profiles by lower degree polynomials has then been investigated. Resort has been made to parabolic velocity profiles and third degree polynomials for the shear. An approach which utilizes the integration of the momentum equation in the three steps from 0 to $\delta_1/2$, from 0 to $\delta_2/2$ and from δ_1 to δ_2 was then established and coupled to an integral solution of the turbulent kinetic energy equation from δ_1 to δ_2. This system was found to be stable even for the case of severe asymmetries between the velocities $u_1(s)$ and $u_2(s)$. It was also found to be as accurate as the previous system based on polynomials of third degree for the velocity, in those cases where the latter system gave stable solutions.

The details of the formulation are as follows. A restricted Dorodnitsyn-Howarth compressibility transformation (where only the n coordinate is stretched) is first invoked, see Appendix A, to yield the transformed momentum equation (barred quantities identify the transformed variables)

$$\bar{u} \ \frac{\partial \bar{u}}{\partial \bar{s}} + \bar{v} \ \frac{\partial \bar{u}}{\partial \bar{n}} = - \ \frac{1}{\rho} \ \frac{\partial \bar{p}}{\partial \bar{s}} + \frac{1}{\rho} \ \frac{\partial \bar{\tau}}{\partial \bar{n}} \ . \tag{1}$$

The velocity profiles are described by a second degree polynomial

$$\bar{u} = \bar{u}_o + a_1 \bar{n} + a_2 \bar{n}^2 \tag{2}$$

and the shear profile by a third degree polynomial

$$\bar{\bar{\tau}} = b_0 + b_1 \bar{n} + b_2 \bar{n}^2 + b_3 \bar{n}^3 \tag{3}$$

The coefficients a_1 and a_2 in Equation (2) are defined by satisfying the boundary conditions $\bar{u} = \bar{u}_1$ at $\bar{n} = \bar{\delta}_1$ and $\bar{u} = \bar{u}_2$ at $\bar{n} = \bar{\delta}_2$. The coefficients b_1, b_2 and b_0 of Equation (3) are obtained by satisfying the conditions $\bar{\tau} = 0$ at $\bar{n} = \bar{\delta}_1$ and $\bar{n} = \bar{\delta}_2$ and by satisfying the s-momentum equation along the base *streamline*.

A Crocco integral, see Appendix A, for the definition of the density variation across the viscous layer is then assumed to be locally valid. In addition, a linear variation of the pressure across the jet can be proved, see Appendix B, to be adequate even in the case of highly curved jets. The integration of the momentum equation, Equation (1), between 0 and $\bar{\delta}_1/2$, 0 and $\bar{\delta}_2/2$ and between δ_1 and δ_2 can then be carried out, see Appendix B, to yield the system of equations

$$\begin{vmatrix} A_{11} & A_{12} & A_{13} \\ A_{21} & A_{22} & A_{23} \\ A_{31} & A_{32} & A_{33} \end{vmatrix} \begin{vmatrix} d\bar{u}_0/ds \\ d\bar{\delta}_1/ds \\ d\bar{\delta}_2/ds \end{vmatrix} = \begin{vmatrix} C_1 \\ C_2 \\ C_3 \end{vmatrix} \tag{4}$$

in the variables $\bar{u}_o$, $\bar{\delta}_1$ and $\bar{\delta}_2$. The coefficients $A_{i,j}$ are functions of $\bar{u}_0$, $\bar{\delta}_1$, $\bar{\delta}_2$, $\bar{u}_1$ and $\bar{u}_2$. The coefficents C_i are functions also of the values of the shear at $n = 0$, $\bar{\delta}_1/2$ and $\bar{\delta}_2/2$, and thus of the coefficient b_3 of Equation (3). The coefficient b_3 is obtained by integrating the turbulent kinetic

energy, TKE, equation across the jet.

It was shown in Reference (12) that the compressible TKE equation of Bradshaw and Ferris[16] can be transformed by the Dorodnitsyn-Howarth transformation into the incompressible form given in Reference (15) and that such an equation, derived originally for boundary layer flows, can be also applied to wakes. The applicability of this equation to straight and curved jet is now assumed. Thus, integration between $\bar{\delta}_1$ and $\bar{\delta}_2$ of the equation

$$\bar{u} \; \frac{\partial}{\partial \bar{s}} \left(\frac{\bar{\tau}}{2a_i \bar{\rho}}\right) + \bar{v} \; \frac{\partial}{\partial \bar{n}} \left(\frac{\bar{\tau}}{2a_i \bar{\rho}}\right) - \frac{\bar{\tau}}{\bar{\rho}} \frac{\partial \bar{u}}{\partial \bar{n}} + \left(\frac{\bar{\tau}_{max}}{\bar{\rho}}\right)^{1/2} \frac{\partial}{\partial \bar{n}} \left(G \frac{\bar{\tau}}{\bar{\rho}}\right) + \frac{(\bar{\tau}/\bar{\delta})^{3/2}}{\bar{L}} = 0 \quad (5)$$

yields, as shown in Appendix B, an equation for b_3 of the form

$$B_1 \; \frac{db_3}{ds} = G_1 \tag{6}$$

Equations (4) and (6) provide the closure of the system of equations and unknowns. Application of the transformation in an inverse manner provides, finally, the desired flow quantities in the physical plane.

SECTION III

COUPLING PROCEDURE FOR COMPLETE SOLUTION

A viscous-inviscid coupling procedure which accounts for strong interaction along the wing and the jet is now developed. The boundary layer solution along the wing is the one developed in Reference (12). The viscous solution along the jet was presented in the preceding section. The details of the initial conditions at the wing trailing edge, where the boundary layer flow merges with the jet flow, are disregarded. The occurance of separation and of recirculation regions at the trailing edge are excluded; however, initial jet profiles are chosen such that the mass and momentum flux of the jet-boundary layer combination is conserved. The viscous analyses are coupled with a relaxation solution of the external inviscid flow. The inviscid solution used here resembles that of Ives and Melnick[6] and is briefly reviewed in order to introduce, in a sequential manner, the description of the coupling.

A schematic representation of the inviscid airfoil/jet flap combination with related nomenclature is shown in Figure (2). Solutions for the flow field in the inviscid limit are sought by numerical integration of the full isentropic, compressible flow equations written in terms of the perturbation potential ϕ, scaled by the freestream velocity and chord, and arranged in the canonical form

$$(1 - q^2/a^2) \ \phi_{ss} + \phi_{nn} = 0 \tag{7}$$

where s and n are othogonal streamline coordinates, a is the local sound speed and q is the total velocity.

For the inviscid problem the boundary conditions along the airfoil and along the jet are, respectively, (it will be seen below that the coupling procedure will manifest itself only in a change in boundary conditions)

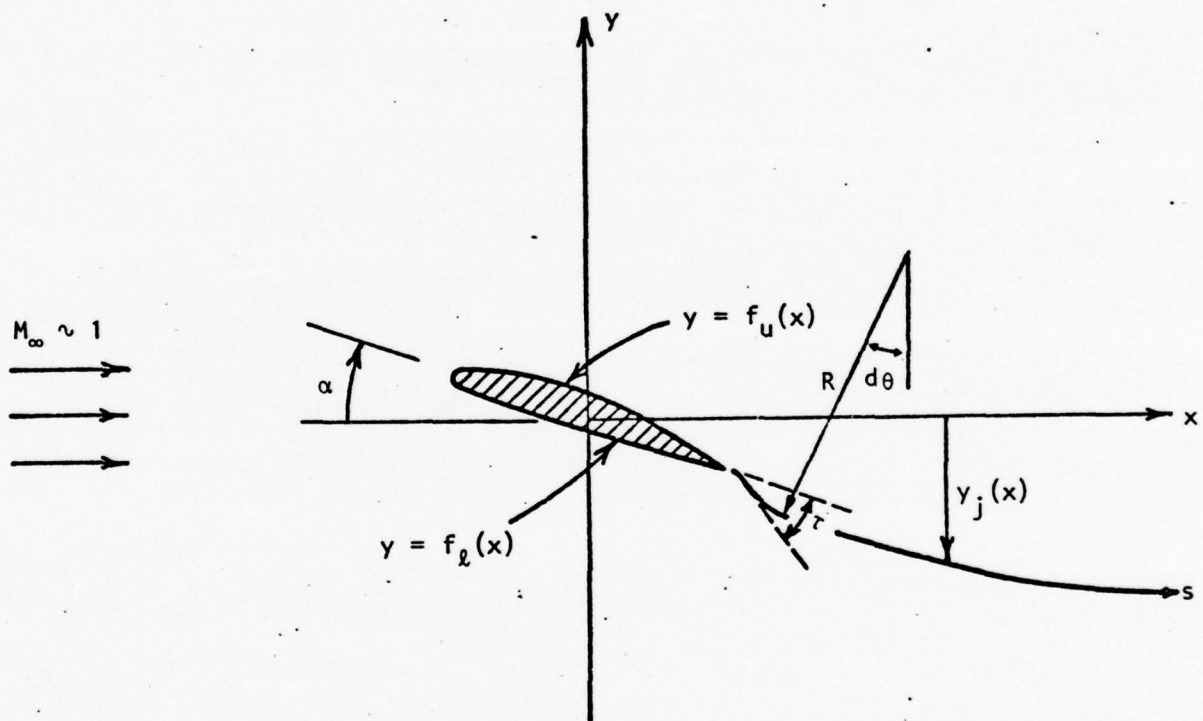$$[\phi_y/(1 + \phi_x)]_{\ell,u} = f'_{\ell,u}(x) \tag{8}$$

FIGURE 2. SCHEMATIC REPRESENTATION OF THE INVISCID JET-FLAPPED AIRFOIL

and

$$[\phi_y/(1 + \phi_x)]_j = y_j'(x). \tag{9}$$

Also, the pressure difference across the jet is required to satisfy the centrifugal force balance

$$\Delta c_p = -c_j/R \tag{10}$$

where c_j is the jet momentum per unit width (divided by the free stream dynamic pressure $1/2 \rho_\infty U_\infty^2$ times the airfoil chord c) and R is the dimensionless (scaled to c) radius of curvature of the jet. Finally, boundary conditions are imposed at infinity. For $M_\infty < 1$, when the problem is inherently elliptic, the standard linearized vortex solution is imposed on the far field potential, viz.

$$\phi_\infty = -\frac{(\Gamma_a + \Gamma_j)}{2\pi} \tan^{-1} \frac{y_\infty \sqrt{1 - M_\infty^2}}{x_\infty} \tag{11}$$

where Γ_a is the circulation about the airfoil and Γ_j is the circulation about the jet sheet.

To numerically solve the system (7) - (11), a transformation from physical space into a unit square is performed. The mapping functions are

$$\xi = \tanh (\alpha_1 x) \tag{12}$$

$$\eta = \tanh \{\alpha_2 [y - g(x)]\}$$

where

$$g(x) = \begin{cases} y_{L.E.} & \text{for } x < x_{L.E} \\ f_u(x) & \text{for } x_{L.E.} < x < x_{T.E.}, \ y > f_u(x) \\ f_\ell(x) & \text{for } x_{L.E.} < x < x_{T.E.}, \ y < f_\ell(x) \\ y_j(x) & \text{for } x > x_{T.E.} \end{cases}$$

A schematic representation of the computational plane is shown in Figure (3).

The solution of Equation (7) is performed in ξ, η using the rotated difference technique of Jameson[17]. Tridiagonal equations of the form

$$a\phi_{i,j-1} + b\phi_{i,j} + c\phi_{i,j+1} = d \tag{13}$$

are derived, where a, b, c and d are functions of the coordinates and the previous iteration values.

The jet boundary condition, Equation (10), is incorporated into the difference scheme following the approach of Ives and Melnick. Across the jet

$$\phi_T = \phi_B + \Gamma(s) \tag{14}$$

where the subscripts T and B denote the top and bottom of the jet sheet, respectively, and Γ denotes the circulation at a given streamwise station along the jet. Since

$$\frac{d\Gamma}{ds} = q_T - q_B$$

and

$$ds = Rd\theta$$

Equation (14) can be combined with Equation (10) and integrated to yield

$$\Gamma_j = \Gamma_{TE} + c_j \int_{\theta_{TE}}^{\theta} \left[\frac{q_T - q_B}{c_{p_B} - c_{p_T}} \right] d\theta \tag{15}$$

Accordingly, the finite difference approximation to Equation (7) just below and just above the jet becomes
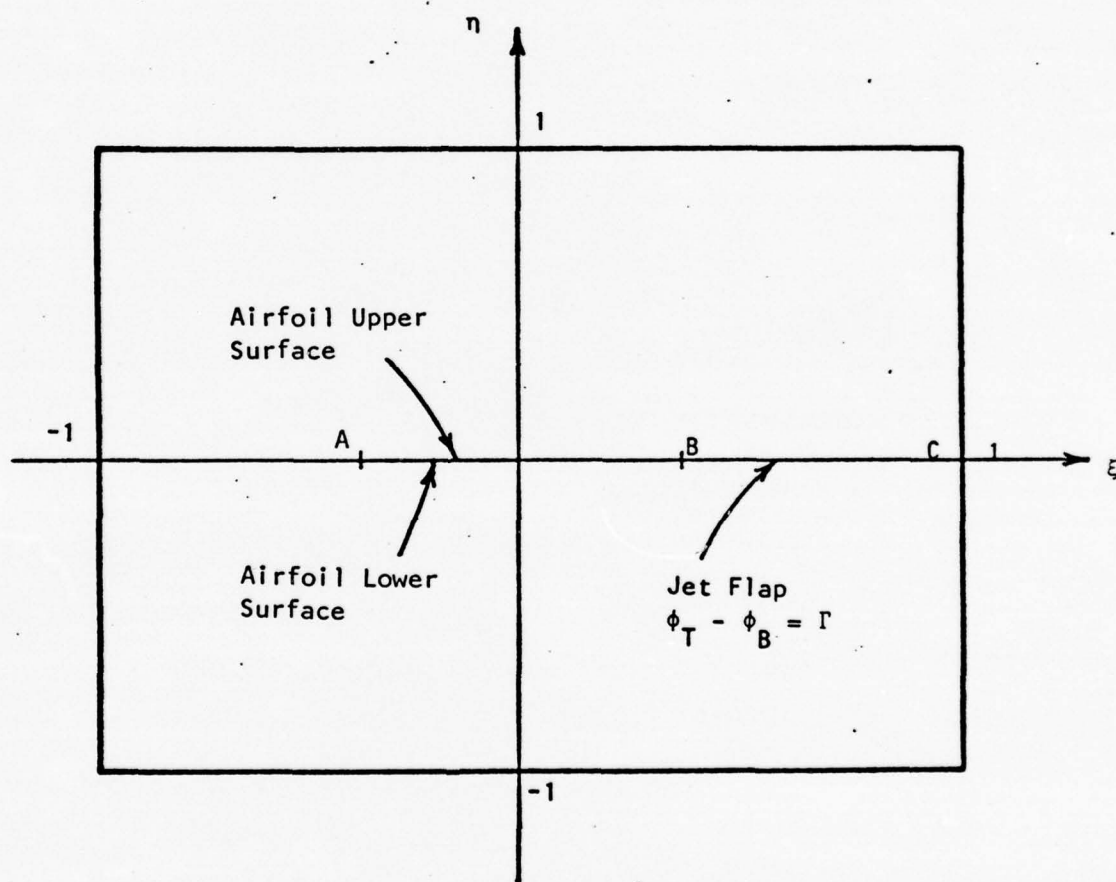
FIGURE 3. SCHEMATIC OF THE ξ, η COMPUTATIONAL PLANE

$$a_B \; \phi_{i,j-1} \; + \; b_B \; \phi_{i,j_B} \; + \; c_B \; \phi_{i,j+1_B} \; = \; d_B$$

$$a_T \; \phi_{i,j-1_T} \; + \; b_T \; \phi_{i,j_T} \; + \; c_T \; \phi_{i,j+1} \; = \; d_T$$

(16)

where $\phi_{i,j+1_B}$ and $\phi_{i,j-1_T}$ are fictitious points outside the flow field, and where ϕ_{i,j_B} and ϕ_{i,j_T} are the values of the potential just below and just above the jet, respectively.

The requirement that the velocity normal to the jet sheet is continuous across the sheet yields an additional relation which, once combined with Equations (15) and (16), eliminates the fictitious potentials $\phi_{i,j+1_B}$ and $\phi_{i,j-1_T}$. Thus, the difference formulation

$$a_T \left(1 + \frac{a_B}{c_B}\right) \; \phi_{i,j-1} + \left(b_T + \frac{b_B \; a_T}{c_B}\right) \phi_{i,j} + (a_T + c_T) \; \phi_{i,j+1} \; =$$

(17)

$$\frac{a_T \; d_B}{c_B} + d_T - b_T \; \Gamma_j + a_T \quad \frac{\alpha_1}{\alpha_2} \; \Delta\eta \; (1 - \xi^2) \; \sin2\theta \; (\phi_T - \phi_B)_\xi$$

valid along the jet flap is achieved. The jet shape is obtained by tracing the streamline coming off the airfoil trailing edge and is updated during each interaction.

The coupling of the viscous results to the inviscid analysis is accomplished by a modification of the boundary conditions along the airfoil (Equation 8) and the jet (Equations 10 and 17). For the flow over the wing, a strong interaction coupling is utilized. The integral of the continuity equation in the viscous region yields

$$\frac{v_e}{u_e} \; = \; \frac{d\delta^*}{dx} \; - \; (\delta - \delta^*) \; \frac{d \; \ln(\rho_e u_e)}{dx} \; .$$

(18)

In addition, as shown in Reference (11), one can express the displacement distribution in the form

$$\frac{d\delta^*}{dx} = \beta_1 + \beta_0 \frac{d \ln(\rho_e u_e)}{dx} \tag{19}$$

(where β_0 and β_1 are functions of the boundary layer quantities c_f, π, δ^* for attached flow and P and δ^* for separated flows, see References 11 and 12). Combining Equations (18) and (19) yields

$$\frac{v_e}{u_e} = \beta_1 + \beta_2 \frac{d \ln(\rho_e u_e)}{dx}$$

where $\beta_2 = \beta_0 - (\delta - \delta^*)$. Thus, the inviscid flow boundary condition

$$\phi_y \simeq f'(x)$$

on the surface of the airfoil with profile $y = f(x)$ is replaced by

$$\phi_y = f'(x) + \beta_1 + \beta_3 \phi_{xx}, \tag{20}$$

where $\beta_3 \simeq \beta_2 (1 + M_\infty^2)$, along the line $y = f(x) + \delta^*(x)$, or by the condition

$$\phi_y^\nu - \beta_3^{\nu-1} \phi_{xx}^\nu = f' + \beta_1^{\nu-1}$$

where the superscript ν denotes the current iteration step. The coupling of inviscid and viscous flows is provided by the coefficients β_1 and β_2 and by the distribution $\delta^*(x)$ (through the positioning of the boundary condition) which are functions of the boundary layer properties (but not of their gradients). This method of coupling is similar in philosphy to that of Tai[18] in that the viscous effect on displacement (through the variable v_e) is directly incorporated into the solution for the inviscid field. It is also noted that in the "full" solution of the Navier-Stokes equations, Diewart[19] utilizes the

flow velocity v_e at the edge of the "viscous" layer directly to determine the outer flow properties.

With regard to the viscous-inviscid interaction along the jet, the two effects of momentum and mass entrainment must be recognized and incorporated directly into the coupling procedure. The first modifies the definition of c_j. The second is the sink effect and implies a discontinuity of normal velocity across the viscous jet. To determine the effect of entrainment on the jet momentum consider the equation for pressure across the jet

$$\frac{\partial p}{\partial n} = - \rho u^2/R$$

and integrate it (in inner viscous variables) to yield

$$\Delta p \left|_{-\infty}^{\infty}\right. = - \int_{-\infty}^{\infty} \frac{\rho u^2}{R} \, dn \quad .$$

But, from the outer (inviscid) solution

$$P_\infty = P_1 + \left(\frac{\partial p}{\partial n}\right)_1 n_\infty + \cdots$$

$$P_{-\infty} = P_2 + \left(\frac{\partial p}{\partial n}\right)_2 n_{-\infty} + \cdots$$

where

$$\left(\frac{\partial p}{\partial n}\right)_1 = - \rho_1 u_1^2/R$$

$$\left(\frac{\partial p}{\partial n}\right)_2 = - \rho_2 u_2^2/R \, .$$

Thus, the effect of mixing on the pressure difference across the jet can be expressed by the relationship

$$\Delta c_p = -\frac{1}{R} \left\{ \int_{\delta_2}^{0} \frac{(\rho u^2 - \rho_2 u_2^2)}{\rho_\infty U_\infty^2 / 2} \, dn + \int_{0}^{\delta_1} \frac{(\rho u^2 - \rho_1 u_1^2)}{\rho_\infty U_\infty^2 / 2} \, dn \right\}$$

which replaces Equation (10). Note that for $\rho u^2 \gg \rho_1 u_1^2$, $\rho_2 u_2^2$, this expression reduces in the inviscid limit to $\Delta c_p = -c_j / R$. Then, if an "effective" momentum coefficient $\overline{c}_j$ is defined, viz.

$$\overline{c_j}(s) = \int_{\delta_2}^{0} \frac{(\rho u^2 - \rho_2 u_2^2)}{\rho_\infty U_\infty^2 / 2} \, dn + \int_{0}^{\delta_1} \frac{(\rho u^2 - \rho_1 u_1^2)}{\rho_\infty U_\infty^2 / 2} \, dn,$$

Equation (15) can be replaced by

$$\Gamma_j^\nu = \Gamma_{T.E.}^\nu + \int_{\theta_{T.E.}}^{\theta} \frac{\overline{c_j}^{\,\nu-1}(s) \, (q_T^\nu - q_B^\nu)}{(c_{p_B}^\nu - c_{p_T}^\nu)} \, d\theta \tag{21}$$

to account for momentum entrainment.

The sink effect is accounted for by imposing along the jet baseline the normal velocity discontinuity

$$(\overline{\Delta v})^\nu = v_{\delta_2}^{\nu-1} - v_{\delta_1}^{\nu-1} \tag{22}$$

where v_{δ_2} and v_{δ_1} are obtained by integrating the continuity equation from the base streamline. Thus

$$\left(\frac{v}{u}\right)_{\delta_2} = \frac{d\,\delta_2{}^*}{ds} - (\delta_2 - \delta_2{}^*)\,\frac{d\,\ell n(\rho_2 u_2)}{ds} \tag{23}$$

$$\left(\frac{v}{u}\right)_{\delta_1} = \frac{d\,\delta_1{}^*}{ds} - (\delta_1 - \delta_1{}^*)\,\frac{d\,\ell n(\rho_1 u_1)}{ds}$$

where

$$\delta_1{}^* = \int_0^{\delta_1} \left(1 - \frac{\rho u}{\rho_1 u_1}\right)\,dn$$

$$\delta_2{}^* = \int_0^{\delta_2} \left(1 - \frac{\rho u}{\rho_2 u_2}\right)\,dn$$

The finite difference form of the transonic equation, Equation (17), along the jet baseline then becomes

$$a_T \left(1 + \frac{a_B}{c_B}\right)\,\phi_{i,j-1} + \left(b_T + \frac{d_B a_T}{c_B}\right)\,\phi_{i,j} + (a_T + c_T)\,\phi_{i,j+1} =$$

$$\frac{a_T d_B}{c_B} + d_T - b_T\,\Gamma_j + a_T\,\frac{\alpha_1}{\alpha_2}\,\Delta\eta\,(1 - \xi^2)\,\sin 2\theta\,(\phi_T - \phi_B)_\xi \tag{24}$$

$$- 2a_T\,\cos\theta\,\frac{\Delta\eta}{\alpha_2}\,\overline{\Delta v}$$

where Γ_j and $\overline{\Delta v}$ are given by Equations (21) and (22), respectively, in terms of values established at a preceding viscous iteration step.

The replacement of Equations (8) and (17) with Equations (20) and (24) constitutes the entire change in the inviscid program to account for strong

viscous interaction. The effects of viscosity are contained in the coefficient β_1 and β_3 of Equation (20) and the coefficients $\overline{c_j}$ and $\overline{\Delta v}$ of Equations (21) and (22). The values of these coefficients are obtained from the viscous analysis along the airfoil and along the jet, developed in Reference (12) and in the present report.

SECTION IV
RESULTS AND CONCLUSIONS

In Reference (11), preliminary results were reported to ascertain the importance of viscous effects in the analysis of jet-flapped airfoils in the transonic regime. For the airfoil without a jet flap the viscous interaction model along the airfoil was validated by the results shown in Figure (4) relative to a 6% circular-arc airfoil at $M_\infty = 0.908$. The numerical result agree quite favorably with the experiment of Reference (20). The influence of jet mixing on the pressure distribution over the wing can be of equal importance, as manifested by the result of Figure (5) which presents the pressure distribution over an airfoil at zero angle of attack without and with a straight jet flap. Additional results have now been obtained by use of the analysis developed in the previous sections.

The influence of mass and momentum entrained by the jet on the pressure distribution over an airfoil was studied by examining the flow about a 12% thick circular-arc airfoil (which is similar to a NACA 0012 except at the nose) at zero angle of attack with a jet flap having an initial deflection angle of 30°, a jet-momentum coefficient $c_j = 0.1$ and a mass flow rate $\rho_j u_j \delta_j / \rho_\infty U_\infty c = 0.04$, at a free stream Mach number of 0.7. Figure (6) presents the pressure distribution over the airfoil for the case of an inviscid, infinitely thin jet flap and of a viscous jet flap. For the viscous jet, the pressure distribution along the upper and lower jet boundaries are given in Figure (7). Also shown in the figure are the corresponding components of the normal velocity as computed by Equation (23) of the viscous analysis. Note that for this case (a moderate c_j and a moderate deflection angle), the sink effect near the trailing edge changes the initial deflection angle by about 6% (since $\tan 30^\circ = 0.577$ and $(\frac{v}{u})_{max} \sim 0.034$). Note also that this effects damps quickly to extremely small values in a distance of about 20% of the chord.

The results of Figure (6) indicate that the pressure distribution on the top-aft section of the airfoil is slightly altered, while that on the bottom-aft section is essentially unaffected. The lower pressure on the aft-top surface results in a decrease in thrust, as compared with the inviscid case, while the
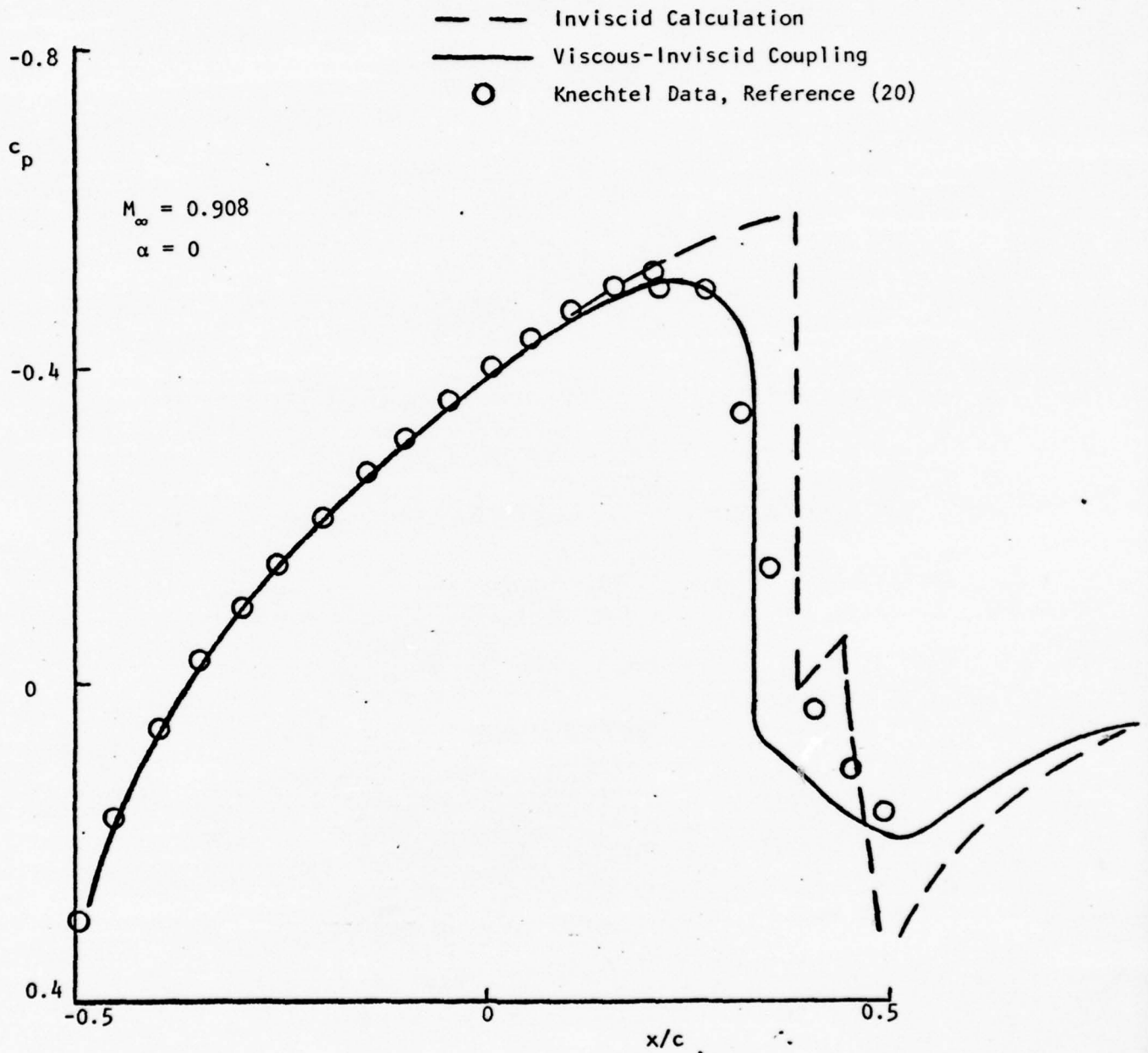
FIGURE 4. EFFECTS OF VISCOUS-INVISCID INTERACTION ON 6% CIRCULAR-ARC AIRFOIL
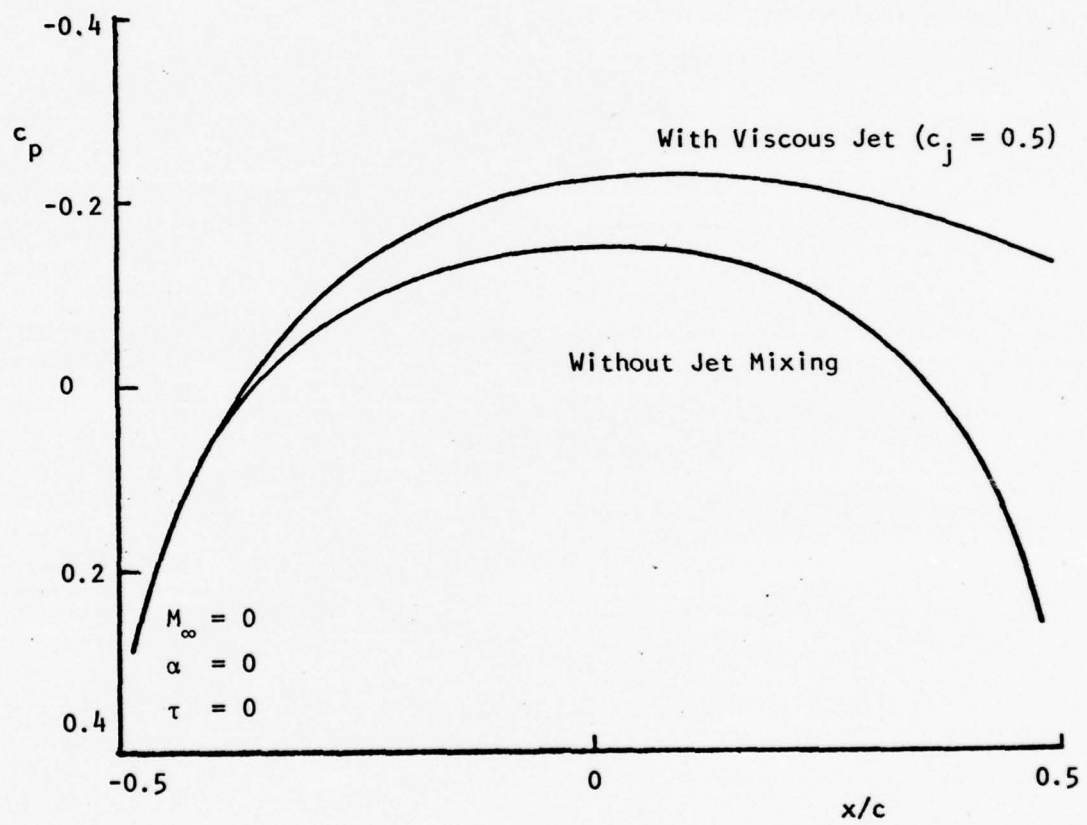
FIGURE 5. EFFECT OF JET MIXING ON PRESSURE DISTRIBUTION OVER A
6% CIRCULAR-ARC AIRFOIL
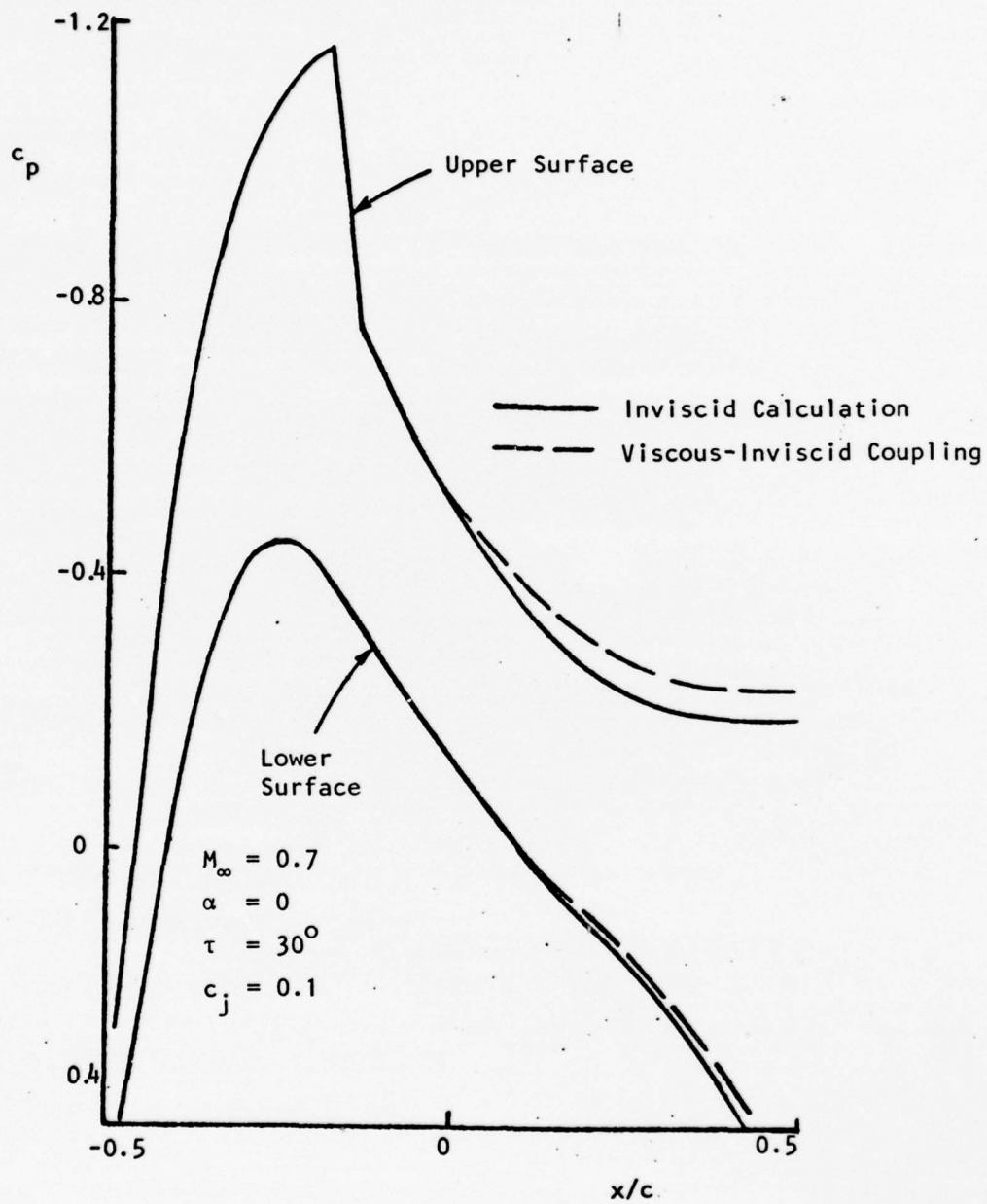
FIGURE 6. EFFECT OF JET VISCOSITY ON PRESSURE DISTRIBUTION OVER A
12% CIRCULAR-ARC AIRFOIL
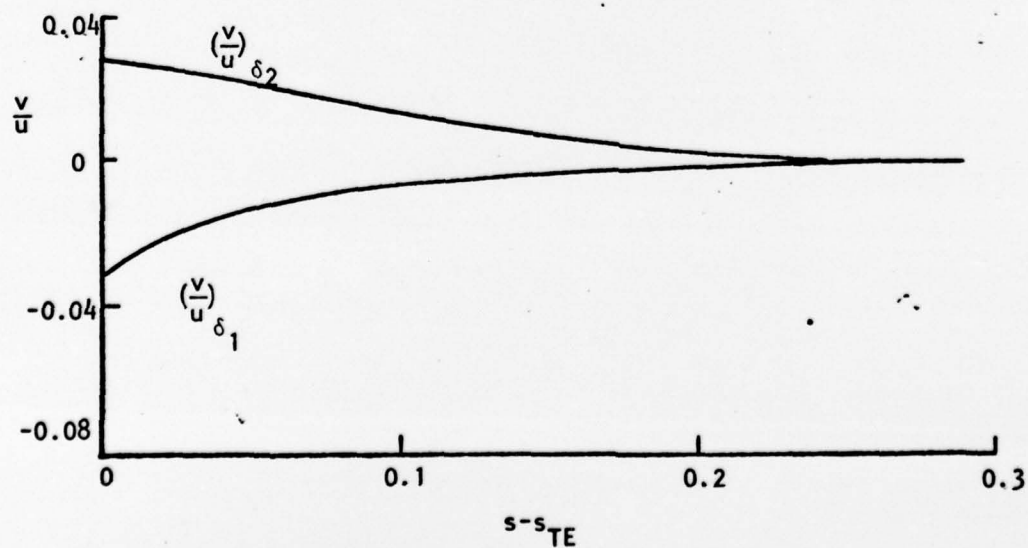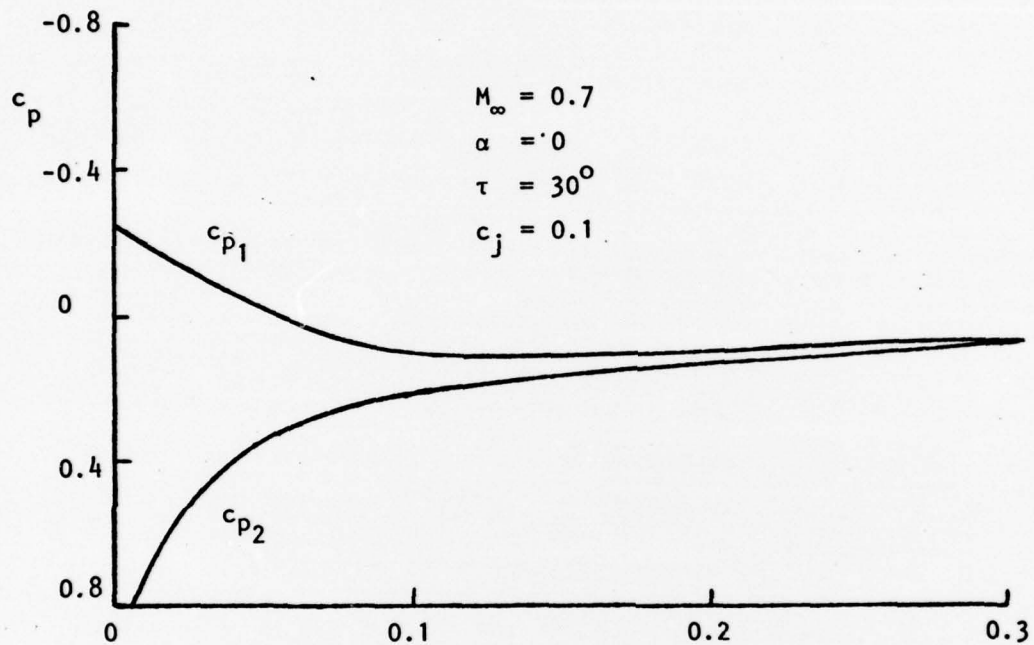
FIGURE 7. PRESSURES AND NORMAL VELOCITIES ALONG BOUNDARIES OF JET
MIXING REGION

lift is somewhat enhanced. The calculation also indicates that, for this parti-
cular case, the effect of momentum entrainment by the jet is small and, to first
order, the jet momentum as a function of position (e.g. the $\overline{c_j}(s)$ coefficient
in Equation (21))is approximatley equal to the initial jet momentum c_j. This
fact may not be true for much smaller values of c_j, i.e. for $c_j << 0.1$. The
major effect of entrainment is due to the sink effect (the parameter Δv of
Equation (22))whose magnitude can be ascertained from Figure (7). The effect of
jet entrainment is more pronounced on the airfoil upper surface than on the low-
er surface, since the flow around the lower surface must experience a large pres-
sure increase near the trailing edge because of the initial jet deflection,
while the upper surface exhibits a relief on adverse gradient due to the jet.
The top surface is also more susceptible to the ejector effect of the jet flap.
In addition, the sink effect is proportional to the magnitude of c_j as indicated
by numerical experiments carried with the present analysis. Thus, for a given
initial jet deflection angle the effect of viscosity, through mass entrainment,
increases with increasing jet momentum.

The other parameter whose variation can significantly alter the effect of en-
trainment is the initial jet deflection angle τ. As τ increases, the inviscid
effects of rear stagnation on the bottom surface and of pressure relief on the
top surface become more and more pronounced. At the same time, the effect of
the jet on separation and bubble development is enhanced. Thus, as pointed
out in Reference (10), the identity of the jet can be obliterated by viscous
mixing. It therefore seems that the effect of viscosity is important for small
(see Figure 5) and large (see Reference 10) jet deflection angles. Thus, one
can expect the effects of entrainment will be most significant for large c_j
and for both small and large τ. Therefore, a program which computes the
viscous-inviscid interaction is necessary to properly ascertain the lift and
thrust increments (or decrements) under a particular set of conditions. The
coupling procedure described in the previous section for the airfoil and the
jet, when utilized in concert, can adequately describe the effects of viscosity
and can be readily incorporated into existing codes for an assessment of jet
flap performance for flows without large separation. In addition, as pointed
out in Reference (10), a proper assessment of viscous effects for the treatment

of jet-flapped wings of finite span would entail the development of a three-dimensional analysis, perhaps utilizing some of the concepts developed herein.

REFERENCES

1. Yoshihara, H., Zonars, D. and Carter, W., "High Reynolds Number Transonic Performance of Advanced Planar Airfoils with Jet-Flaps," AFFDL TR 71-61, June 1971.

2. Peake, D., Yoshihara, H., Zonars, D. and Carter, W., "The Transonic Performance of 2D Flapped Aerofoils at High Reynolds Numbers," AGARD CP No. 83, August 1971.

3. Yoshihara, H., Magnus, R. and Zonars, D., "Transonic Drag due to Lift of Planar Jet-Flapped Airfoils," AGARD CP No. 124, 1973.

4. Yoshihara, H., Benepe, D. and Whidden, P., "Transonic Performance of Jet-Flaps on Advanced Fighter Configuration," AFFDL TR-73-97, 1973.

5. Peake, D. J., Bowker, A. J., Mokry, M., Yoshihara, H. and Magnus, R, "Transonic Lift Augmentation of Two-Dimensional Supercritical Aerofoils by Means of Aft Camber, Slot Blowing and Jet-Flaps, in High Reynolds Number Flow," ICAS Paper No. 74-11, Haifa, Israel, August 1974.

6. Ives, D. D. and Melnick, R. E., "Numerical Calculation of the Compressible Flow over an Airfoil with a Jet-Flap," AIAA Paper No. 74-542, June 1974.

7. Malmuth, N. D. and Murphy, W. D., "A Relaxation Solution for Transonic Flow over Jet-Flapped Airfoils," AIAA Journal, Vol. 14, No. 9 September 1976.

8. Malmuth, N. D. and Murphy, W. D., "Relaxation Solution for Transonic Flow over Three-Dimensional Jet-Flapped Wings," AIAA Journal, Vol. 15, No. 1, January 1977.

9. Stratford, B. S., "Mixing and the Jet-Flap," The Aeronautical Quarterly, Vol. VII, 1956.

10. Yoshihara, H. and Zonars, D., "The Transonic Jet Flap - A Review of Recent Results," SAE Transactions, Vol. 84, Section 4, Paper No. 75189, 1975.

11. Elzweig, S., Baronti, P. and Miller, G., "An Analysis of Transonic Jet-Flapped Airfoils with the Inclusion of Viscous Effects," ATL TR 230, May 1976.

12. Miller, G. and Baronti, P., "Solution of Transonic Separating Turbulent Boundary Layers," ATL TR 214, May 1975.

13. Baronti, P. and Miller, G., "Integral Solution of the Turbulent Kinetic Energy Equation," AIAA Journal, Vol. 12, No. 1, January 1974.

14. Ting, L., "On the Mixing of Two Parallel Streams," Journal of Mathematical Physics, Vol. 38, No. 3, October 1959.

REFERENCES (Continued)

15. Bradshaw, P., Ferris, D. H. and Atwell, N. P., "Calculation of Boundary Layer Development Using the Turbulent Energy Equation," Journal of Fluid Mechanics, Vol. 28, Part 3, 1967.

16. Bradshaw, P. and Ferris, D. H., "Calculation of Boundary-Layer Development Using the Turbulent Energy Equation: Compressible Flow on Adiabatic Walls," Journal of Fluid Mechanics, Vol. 46, Part 1, 1971.

17. Jameson, A., "Transonic Potential Flow Calculations Using Conservation Form," Procs. AIAA 2nd Computational Fluid Dynamics Conference, Hartford, CT, June 1975.

18. Tai, T. C., "Transonic Turbulent Viscous-Inviscid Interaction over Airfoils," AIAA Paper No. 75-78, January 1975.

19. Deiwert, G. S., "Numerical Simulation of High Reynolds Number Transonic Flows," AIAA Journal, Vol. 13, No. 10, October 1975.,

20. Knechtel, E. D., "Experimental Investigation at Transonic Speeds of Pressure Distributions over Wedge and Circular-Arc Airfoil Sections and Evaluation of Perforated-Wall Interference," NASA TN-D-15, August 1959.

TR 237

APPENDIX A

COMPRESSIBILITY TRANSFORMATIONS AND CROCCO

RELATION FOR VISCOUS JET ANALYSIS

A restricted Dorodnitsyn-Howarth transformation

$$\bar{s} = s$$

$$\bar{n} = \int_0^n \rho/\bar{\rho} \; dn \qquad\qquad (A,1)$$

$$\bar{\psi} = \psi$$

with barred quantities denoting transformed values, is utilized here to account for compressibility effects along the jet.

The transformation implies that

$$\bar{u} = u$$

and

$$\bar{v} = \frac{v\rho}{\bar{\rho}} + \bar{u} \frac{\partial \bar{n}}{\partial s}$$

Then, if it is further assumed that $\tau = \bar{\tau}$, the momentum equation along the jet becomes (to order δ)

$$\bar{u} \; \frac{\partial \bar{u}}{\partial \bar{s}} + \bar{v} \; \frac{\partial \bar{n}}{\partial \bar{n}} = -\frac{1}{\rho} \; \frac{\partial p}{\partial \bar{s}} + \frac{1}{\bar{\rho}} \; \frac{\partial \bar{\tau}}{\partial \bar{n}} \qquad\qquad (A,2)$$

Since across the jet

$$\frac{\partial p}{\partial n} = -\rho \; \frac{u^2}{R} \quad,$$

application of the transformation also implies

A1

$$\frac{\partial p}{\partial \bar{n}} = -\frac{\overline{\rho u}^2}{R} \qquad (A,3)$$

and thus

$$\frac{\partial p}{\partial \bar{n}} = \frac{\partial \bar{p}}{\partial \bar{n}} \quad .$$

It then also follows that

$$\frac{\partial \bar{p}}{\partial \bar{s}} = \frac{\partial \bar{p}}{\partial \bar{s}} = \frac{\partial p}{\partial s}$$

The density term $1/\rho$ in the momentum equation can be expressed directly in terms of velocity and pressure profiles and of edge conditions by invoking the local validity of the Crocco integral. One then has

$$\frac{1}{\rho} = \frac{1}{p} \quad [Au + B - \frac{\gamma-1}{2\gamma} u^2] \qquad (A,4)$$

where

$$A = \frac{(p_1/\rho_1 - p_2/\rho_2)}{u_1 - u_2} + \frac{\gamma-1}{2\gamma} (u_1 + u_2)$$

$$B = \frac{(p_2/\rho_2 \, u_1 - p_1/\rho_1 \, u_2)}{u_1 - u_2} - \frac{\gamma-1}{2\gamma} u_1 u_2 .$$

APPENDIX B

INTEGRAL METHOD FOR CURVED JET

Integration of the transformed momentum equation, Equation (A,2), between 0 and $\bar{\delta}_1/2$, 0 and $\bar{\delta}_2/2$ and between $\bar{\delta}_1$ and $\bar{\delta}_2$ yields (for convenience, all transformed quantities are now indicated by unbarred symbol whereas $\tilde{\rho}$ indicates the compressible density)

$$\frac{d}{ds} \int_0^{\delta_i/2} u^2 \, dn = u_{\delta_i/2} \, \frac{d}{ds} \int_0^{\delta_i/2} u \, dn =$$

$$-\int_0^{\delta_i/2} \frac{1}{\tilde{\rho}} \frac{\partial p}{\partial s} \, dn + (\tau/\rho)_{\delta_i/2} - (\tau/\rho)_0 \tag{B,1}$$

where $i = 1, 2$, and

$$\frac{d}{ds} \int_{\delta_2}^{\delta_1} u^2 \, dn - u_1 \frac{d}{ds} \int_0^{\delta_1} u \, dn + u_2 \, \frac{d}{ds} \int_0^{\delta_2} u \, dn =$$

$$-\int_{\delta_2}^{\delta_1} \frac{1}{\tilde{\rho}} \frac{\partial p}{\partial s} \, dn \tag{B,2}$$

The density $\tilde{\rho}$ has been defined above by Equation (A,4), the velocity profiles are expressed by the polynomial

$$u = u_0 + a_1 n + a_2 n^2 \tag{B,3}$$

where u_0 is the velocity along the "base" streamline and where the coefficients a_1 and a_2 are obtained by satisfying the boundary conditions $u=u_1$ at $n=\delta_1$ and $u=u_2$ at $n=\delta_2$ to yield

$$a_1 = [(u_1 - u_0) \; \delta_2^2 - (u_2 - u_0) \; \delta_1^2]/D$$

$$a_2 = [(u_2 - u_0) \; \delta_1 - (u - u_0) \; \delta_2]/D$$

$$D = \delta_1 \; \delta_2^2 - \delta_2 \; \delta_1^2$$

The pressure distribution across the layer can be obtained by integrating the normal momentum equation (A,3) to yield a fifth-order polynomial for p. This was originally proposed in Reference (11). It was felt, however, that since $\partial p/\partial n$ cannot change sign across the layer, it may be possible to lower the order of the polynomial. Extensive investigation has indicated that a linear solution is adequate. A pressure distribution of the form

$$p = \frac{1}{(\delta_1 - \delta_2)} \; [(p_2 \delta_1 - p_1 \delta_2) + (p_1 - p_2) n] \tag{B,4}$$

has been, henceforth, utilized here.

Thus, by inserting Equations (A,4), (B,3) and (B,4) into Equations (B,1) and (B,2) and performing the integrations and differentiations one obtains the system of equations

$$a_{11} \; \frac{du_0}{ds} + a_{12} \; \frac{d\delta_1}{ds} + a_{13} \; \frac{d\delta_2}{ds} = C_1$$

$$a_{21} \; \frac{du_0}{ds} + a_{22} \; \frac{d\delta_1}{ds} + a_{23} \; \frac{d\delta_2}{ds} = C_2 \tag{B,5}$$

$$a_{31} \; \frac{du_0}{ds} + a_{32} \; \frac{d\delta_1}{ds} + a_{33} \; \frac{d\delta_2}{ds} = C_3$$

which defines the flow variables u_0, δ_1 and δ_2.

To obtain the shear distribution and, thus, the values $\tau_{\delta1/2}$, $\tau_{\delta2/2}$ and τ_0 appearing in Equations (B,1) and (B,2) it is assumed that (unbarred quantities shall indicate transformed values).

$$\tau/\rho = b_0 + b_1 n + b_2 n^2 + b_3 n^3 \tag{B,6}$$

The coefficient b_1 is obtained by satisfying the s-momentum equation along the n = 0 line; hence

$$b_1 = \left(\frac{\partial \tau}{\partial n}\right)_0 = u_0 \frac{du_0}{ds} + \frac{1}{\tilde{\rho}_0} \left(\frac{\partial p}{\partial s}\right)_0$$

The coefficients b_0 and b_2 are obtained by satisfying the boundary conditions

$$\tau = 0 \text{ at } y = \delta_1, \ \delta_2 \ .$$

Hence,

$$b_0 = \frac{1}{D_2} \{-(b_1 \delta_1 + b_3 \delta_1^3) \ \delta_2^2 + (b_1 \delta_2 + b_3 \delta_2^3) \ \delta_1^2\}$$

$$b_2 = \frac{1}{D_2} \{-(b_1 \delta_1 + b_3 \delta_2^3) + (b_1 \delta_1 + b_3 \delta_1^3)\}$$

where

$$D_2 = \delta_2^2 - \delta_1^2$$

The coefficient b_3 is then obtained by integrating the TKE equation (Equation B,5) across the viscous jet layer, viz.,

$$\frac{1}{2a_i} \frac{d}{ds} \int_{\delta_2}^{\delta_1} \frac{\tau}{\rho} \, u \, dn - \int_{\delta_2}^{\delta_1} \frac{\tau}{\rho} \frac{\partial u}{\partial n} \, dn$$

$$\tag{B,7}$$

$$+ \int_{\delta_2}^{\delta_1} \frac{(\tau/\rho)^{3/2}}{L} \, dn = 0$$

B3

with the parameters a_i and L given in Reference (15). By inserting Equations (B,3) and (B,6) into Equation (B,7), on then obtains the ordinary differential equation for b_3 of the form

$$B_1 \frac{db_3}{ds} = G_1$$

Thus, Equations (B,5) and (B,7) provide the sought closure of equations and unknowns for the solution of $\delta_1(s)$, $\delta_2(s)$, $u_0(s)$ and $b_3(s)$ in the transformed plane.

SECURITY CLASSIFICATION OF THIS PAGE (When Data Entered)

REPORT DOCUMENTATION PAGE		READ INSTRUCTIONS BEFORE COMPLETING FORM
1. REPORT NUMBER AFOSR - TR - 77 - 0446	2. GOVT ACCESSION NO.	3. RECIPIENT'S CATALOG NUMBER
4. TITLE (and Subtitle) THE EFFECTS OF VISCOUS INTERACTION ON THE TRANSONIC JET-FLAP		5. TYPE OF REPORT & PERIOD COVERED FINAL rept. 1 Oct 75 — 30 Sep 76
		6. PERFORMING ORG. REPORT NUMBER GASL-TR-237
7. AUTHOR(s) P. BARONTI, S. ELZWEIG G. MILLER		8. CONTRACT OR GRANT NUMBER(s) F44620-76-C-0017
9. PERFORMING ORGANIZATION NAME AND ADDRESS GENERAL APPLIED SCIENCE LABORATORIES, INC. MERRICK AND STEWART AVENUES WESTBURY, NEW YORK 11590		10. PROGRAM ELEMENT, PROJECT, TASK AREA & WORK UNIT NUMBERS 9781-01 61102F
11. CONTROLLING OFFICE NAME AND ADDRESS AIR FORCE OFFICE OF SCIENTIFIC RESEARCH/NA BLDG 410 BOLLING AIR FORCE BASE, D C 20332		12. REPORT DATE March 1977
		13. NUMBER OF PAGES 40
14. MONITORING AGENCY NAME & ADDRESS(if different from Controlling Office)		15. SECURITY CLASS. (of this report) UNCLASSIFIED
		15a. DECLASSIFICATION/DOWNGRADING SCHEDULE

16. DISTRIBUTION STATEMENT (of this Report)

Approved for public release; distribution unlimited.

17. DISTRIBUTION STATEMENT (of the abstract entered in Block 20, if different from Report)

18. SUPPLEMENTARY NOTES

19. KEY WORDS (Continue on reverse side if necessary and identify by block number)
JET FLAPS
TRANSONIC FLOW
VISCOUS-INVISCID INTERACTION

20. ABSTRACT (Continue on reverse side if necessary and identify by block number)
The inviscid and viscous effects associated with a jet-flapped airfoil in the transonic regime are investigated. The particular formulation developed employs integral methods for the description of the viscous portions of the flow (utilizing the turbulent kinetic energy equation) and a relaxation method for the inviscid portions. The viscous-inviscid coupling procedures along the wing and the jet acknowledge the importance and magnitude of the viscous effects on pressure distribution and directly incorporate the displacement effect on the wing and the effects of the jet mixing into the boundary conditions for the computation →

of the entire flow. Some numerical results are presented to validate the solution techniques that have been selected and to assess the importance of mass and momentum entrainment into the jet on jet flap effectiveness.